Optical Power Efficiency Versus Breakdown Voltage of Avalanche-Mode Silicon LEDs in CMOS

Satadal Dutta, *Student Member, IEEE*, Gerard J. M. Wienk,
Raymond J. E. Hueting, *Senior Member, IEEE*,
Jurriaan Schmitz, *Senior Member, IEEE*,
and Anne-Johan Annema, *Member, IEEE*

Abstract—We report on the dependency of the optical power efficiency η on the breakdown voltage V_{BR} of avalanche-mode (AM) light-emitting diodes (LEDs) in silicon. Lateral p^+-n-n^+ LEDs have been designed in a 65-nm bulk CMOS technology, where V_{BR} is varied between 2 and 9 V. This tunes both the magnitude and the spatial distribution of the reverse electric field, which governs AM electroluminescence. Experiments show that a maximum η of $\sim 1.7 \times 10^{-6}$ is obtained for $V_{BR} \sim 6$ V. For $V_{BR} < 6$ V, non-local avalanche results in a lower η, while for $V_{BR} > 6$ V, a gradual reduction in η with increasing V_{BR} is obtained. This trend is compared with two recently proposed opto-electronic models. A maximum in η at relatively low voltages is attractive for monolithic opto-electronic integration in silicon.

Index Terms—Avalanche breakdown, silicon, electroluminescence, LED, power efficiency, internal quantum efficiency.

I. INTRODUCTION

THE avalanche-mode light-emitting diode (AMLED) is a potential candidate as a silicon (Si) based light source for monolithic opto-electronic integration in standard CMOS technology, e.g. optical links [1]–[8], primarily due to the significant overlap between its electroluminescent (EL) spectra and the spectral responsivity of Si photodiodes (PDs) [1], [8]. Avalanche-mode electroluminescence (AM-EL) is governed by impact ionization [9] and hence by the electric field F [10]. The relatively low internal quantum efficiency (IQE) of AMLEDs ($\sim 10^{-5}$) [3] combined with the typical p-n junction breakdown voltages V_{BR} render AM-EL to be significantly power-hungry. Thus, maximizing the optical power efficiency η, defined as the ratio of the optical power P_{opt} to the electrical power P_{LED}, is highly desired. The existence of an optimum
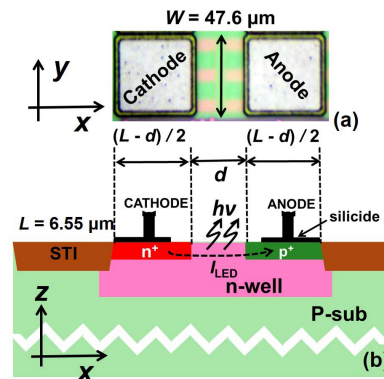
Fig. 1. Schematic (a) top-view and (b) cross-section of the p^+-n-n^+ LED. The spacing d between the p^+ and n^+ regions has been varied in steps of 20 nm.

$V_{BR} \sim 5$ V at which η is maximum was reported earlier [11], based on devices in a BiCMOS process, where measured values of η were fitted with an empirical model. However, the underlying physical mechanism was not explained. Recently, a physics-based opto-electronic model [10] was derived for an abrupt optimized 1-D p^+-n junction (i.e. for a single-sided triangular electric field profile). Here the optical intensity was related to the field-dependent electron temperature (T_e) profile, where an optimal $V_{BR} \sim 5$ V was also theoretically predicted, using a non-local avalanche model [10], [12]–[14]. In addition, there was a lack of enough experimental variation in V_{BR}, especially at low voltages, to verify both models proposed in [10] and [11].

In this work, we report on an experimentally obtained relation between η and V_{BR} using lateral nanometer-scale p^+-n-n^+ junction diodes designed in a standard 65 nm bulk CMOS technology. We vary V_{BR} by geometric scaling of the LED, resulting in a trapezoidal field-profile $F(x)$ for a fixed doping level N determined by the technology. Results are compared with the models of [10] and [11]. We show that our model [10] is in a good agreement with our new experimental data.

II. DESIGN OF THE LED

Fig. 1(a) shows the device top-view and (b) shows the vertical cross-section of the designed p^+-n-n^+ LEDs. Each LED has a fixed total length $L \approx 6.5 \ \mu$m along the
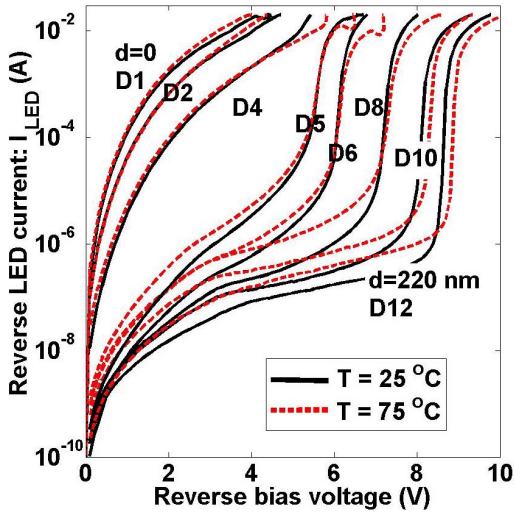
Fig. 2. Measured dc *I-V* characteristics (in dark) of the LEDs D1 to D6, D8, D10, and D12 at $T = 25$ °C and 75 °C. Measurements were done using a Keithley 4200 Semiconductor Characterization System (SCS).

Fig. 3. (a) TCAD simulated field profiles $F(x)$ at breakdown for the indicated LEDs along the white dashed cut-line ($z = -0.1$ μm) shown in the inset. The red dashed line is a guide to the eye for the peak field trend. (Inset): 2-D TCAD simulated electric field profile at breakdown, for $d = 40$ nm. (b) Calculated electron temperature profiles $T_e(x)$ following Eq. (1) for the indicated LEDs. The arrows indicate the direction of the electron and hole current flow.

x-axis, and a fixed width $W = 47.6$ μm along the y-axis. The designed spacing d between the n^+ and p^+ region is varied from $d = 0$ in LED D1 till $d = 280$ nm in LED D15, in steps of 20 nm. D1 is a special case of a p^+-n^+ junction. The silicide layer is avoided along the active region except at the electrode contacts, to enable vertical emergence and detection of light, and to prevent shorting of the junction. Avalanche breakdown, important for AM-EL, initiates via impact ionization that generates electron-hole pairs. Those pairs are swept apart by the high reverse electric field close to the junction and are accelerated to energies in excess of the band-gap. A certain fraction of these high energy electrons recombine with holes leading to isotropic AM-EL [9], [10].

III. OPTO-ELECTRONIC BEHAVIOR

Fig. 2 shows the measured dc reverse I-V characteristics of the LEDs D1 to D6, D8, D10, and D12 with an increasing d, in dark conditions and at ambient temperatures $T = 25$ °C and 75 °C. For $d \leq 60$ nm (D1 to D4), the reverse current I_{LED} has a negligible T-dependence, and a sub-unity ideality factor indicating the presence of band-to-band tunneling (BTBT) [15], [16]. This leads to a "soft" transition into breakdown. For $d > 80$ nm (D6 onwards), the I-V curves show a progressively sharper transition into breakdown, and a more pronounced T-dependence, indicating impact ionization and avalanche breakdown [17].

The V_{BR} of the LEDs is defined at a fixed current $I_{LED} = 1$ mA [18]. The trend in V_{BR} is explained by the 2-D TCAD simulated [19] $F(x)$ at $V \approx V_{BR}$, as shown in Fig. 3(a). The inset of Fig. 3(a) shows a snap-shot of the 2-D field profile for $d = 40$ nm. An effective $N \sim 10^{17}$ cm^{-3} has been obtained by fitting the measured V_{BR} in TCAD. $F(x)$ is trapezoidal for fully depleted short diodes. With increasing d, the peak field F_m rapidly reduces to a value corresponding to that of an abrupt p^+-n junction, while the depletion width increases till its maximum, where $F(x)$ becomes roughly triangular. The AM-EL is dependent on the electron temperature T_e [10], therefore the TCAD simulated
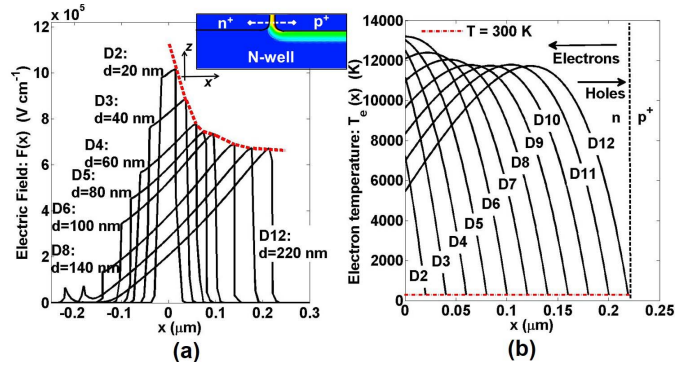
$F(x)$ is used to compute the latter according to:

$$T_e(x) = T + \frac{2q}{5k_B} \int_0^x F(u) \exp\left[\frac{u - x}{\lambda_e}\right] du, \quad 0 \leq x \leq d, \tag{1}$$

where q is the elementary charge, k_B is the Boltzmann constant, and $\lambda_e \propto v_e \cdot \tau_e$ is the mean energy relaxation length for electrons with velocity v_e as defined in [13] and [14], where $\lambda_e = 65$ nm was reported for Si. Here τ_e is the mean inter-scattering time in Si, which depends on T and is governed by acoustic deformation potential (ADP) scattering [20]. The calculated $T_e(x)$ is shown for the indicated LEDs in Fig. 3(b). From D2 to D6 ($d < 2\lambda_e$), the peak T_e first rapidly increases due to non-local avalanche, and then for $d > 2\lambda_e$ it gradually reduces from D7 onwards due to the gradual reduction in F_m.

The peak T_e is used to evaluate the carrier probability distribution functions, which are then used to calculate P_{opt} by integrating all the electron transitions to the valence band edge [10], [21]. Next, we discuss the optical properties of the LEDs.

Fig. 4(a) shows the AM-EL micrographs of the LEDs at $I_{LED} = 5$ mA, captured vertically using a visible range camera. Light emission appears along the line of the junction oriented along the y-axis. The brightness is observed to increase rapidly from D1 to D6, and then saturates from D7 onwards. Fig. 4(b) shows the measured spectral irradiance of D6 ($V_{BR} \approx 6$ V) at various I_{LED}. These EL-spectra (observed in the spectral range of 400 nm $< \lambda <$ 900 nm) have been corrected for the effect of Fabry-Perot interference in the multi-layer back-end dielectric stack, which has been characterized by its spectral transmittance, as shown in Fig. 4(c) using a broad-spectrum halogen lamp from Bausch and Lomb. The EL-spectra exhibit a broad peak centered at $\lambda \sim 620$ nm that can be attributed to phonon-assisted (indirect) inter-band recombination. The emission at $\lambda \gtrsim 700$ nm can also be contributed by intra-band electron transitions, while emission at $\lambda \lesssim 480$ nm can be partly contributed by direct inter-band recombination [22]–[24]. It is worth mentioning that our model [10] only caters to the dominant indirect inter-band recombination; detailed modeling of the other types of transitions requires further study.
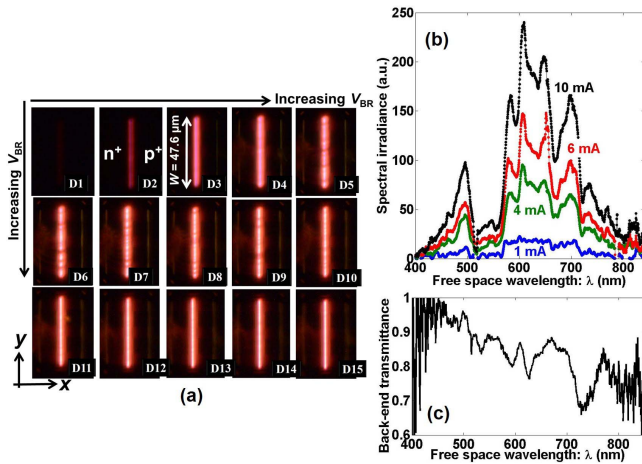
Fig. 4. (a) AM-EL micrographs of the LEDs D1 to D15, each at $I_{LED} = 5$ mA (to the same scale and resolution). Light is captured vertically (out of plane along the z-axis). The images are captured by a visible range camera with a 20 s integration time. (b) Vertically measured EL-spectra of D6 for various I_{LED}, measured using a multi-mode optical fiber feeding an ADC-1000-USB spectrometer from Avantes, with an integration time of 20 s. (c) Spectral transmittance of the back-end stack obtained from reflectance measurement.
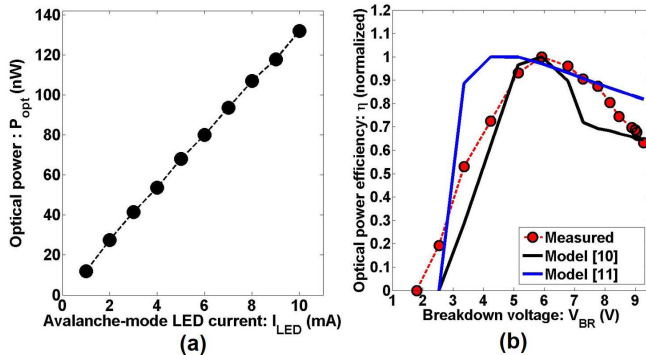

Fig. 5. (a) Emitted optical power of the avalanche-mode LED D6 versus I_{LED}. (b) Normalized optical power efficiency versus V_{BR}, where the experimental trend is compared with those predicted using the 1-D physics-based opto-electronic model [10] and the empirical model [11].

A linear variation in the total optical power P_{opt} emitted by the LEDs with increasing I_{LED} is observed, as shown for D6 in Fig. 5(a), with $\eta = P_{opt}/P_{LED} \approx 1.7 \times 10^{-6}$ and a mean intensity of ~ 28 nW μm^{-2} at $I_{LED} = 10$ mA. P_{opt} has been extracted using an ultra-sensitive, off-chip calibrated photodiode (PD) [25], mounted vertically above of the die, which is done by extracting the emission-specific responsivity of the PD [8]. The external and internal quantum efficiencies (EQE and IQE) of D6 have been estimated to be $\sim 2.0 \times 10^{-8}$ and $\sim 6.0 \times 10^{-6}$, respectively, assuming isotropic light emission [9]. The obtained IQE and EQE values match well with prior results [3], [22], [26].

The same linear variation in P_{opt} versus I_{LED} has been observed by integrating the measured EL-spectra over λ. In Fig. 5(b), η is plotted against V_{BR} of the LEDs, where it is normalized w.r.t. its maximum value (for D6). The normalization is done for comparison with the modeled trends. The trends in η versus V_{BR} for the LEDs, as predicted by the models [10], [11] are also shown in Fig. 5(b). Our model [10] for $\lambda_e = 65$ nm [13] is in better agreement with the measured trend. A maximum η is obtained in our experiment for

$V_{BR} \sim 6$ V. For $V_{BR} < 6$ V, non-local avalanche leads to a rapid decrease in η with decreasing V_{BR} (thus decreasing d) despite an increasing $F_m(d)$. This can be understood as follows: when $d \lesssim \lambda_e$, the electrons do not have sufficient space to be accelerated by the increasing local F_m to high energies. Hence, the peak T_e drops, leading to a drop in P_{opt}.

For $V_{BR} > 6$ V (LEDs D7 to D15), a continuous reduction in η with increasing V_{BR} is obtained. This is due to two phenomena: (a) F_m reduces for increasing d, and (b) the spatial width across which the high field (hence the EL-region) extends along the x-axis becomes narrower as $F(x)$ changes from being trapezoidal to triangular. This is reflected in the increase of V_{BR}, and hence P_{LED}.

The discrepancies between the modeled and measured $\eta - V_{BR}$ curves are likely due to the uncertainties in N, d, and the assumption of a 1-D EL-region in the optical model. Further, BTBT [15], [16], [27] has not been taken into account in the model. BTBT is the most pronounced in D1 (explaining its low P_{opt}), being a p^+-n^+ junction.

The LEDs were further put under an accelerated stress for 30 hours at a dc bias of $I_{LED} = 10$ mA and 100 °C ambient. No degradation in the total P_{opt} has been observed, in line with previous reports of bulk CMOS AMLEDs [28]. However, one can expect hot-carrier induced electrical degradation, due to the high field near the Si-SiO$_2$ interface [29], [30].

As a final remark, η can be enhanced by adopting new LED designs which improve the spatial uniformity of $F(x)$ and consequently P_{opt}, such as the recently reported superjunction AMLEDs [31]. A maximum in η at relatively low voltages is attractive for monolithic integration of Si-based optical functions in standard CMOS.

IV. CONCLUSIONS

The dependency of optical power efficiency η on the breakdown voltage V_{BR} of avalanche-mode (AM) p^+-n-n^+ junction LEDs in silicon, designed in a standard 65 nm bulk CMOS technology, has been shown experimentally and compared with analytical models. Measurements show a maximum η at $V_{BR} \sim 6$ V. For $V_{BR} < 6$ V, a rapid decrease in η is obtained for decreasing V_{BR} despite an increase in the peak electric field. For $V_{BR} > 6$ V, a reduction in η with increasing V_{BR} is obtained due to a gradual reduction in both the magnitude and the spread of the electric field. The measurements are explained with our opto-electronic model that relates AM electroluminescence from Si LEDs to the field-dependent electron temperature based on the non-local avalanche effect.

REFERENCES

[1] B. P. van Drieënhuizen and R. F. Wolffenbuttel, "Optocoupler based on the avalanche light emission in silicon," *Sens. Actuators A, Phys.*, vol. 31, nos. 1–3, pp. 229–240, Mar. 1992, doi: 10.1016/0924-4247(92)80110-O.

[2] M. D. Plessis, H. Aharoni, and L. W. Snyman, "Silicon LEDs fabricated in standard VLSI technology as components for all silicon monolithic integrated optoelectronic systems," *IEEE J. Sel. Topics Quantum Electron.*, vol. 8, no. 6, pp. 1412–1419, Nov. 2002, doi: 10.1109/JSTQE. 2002.806697.

[3] L. W. Snyman, M. du Plessis, and H. Aharoni, "Injection-avalanche-based n$^+$pn silicon complementary metal–oxide–semiconductor light-emitting device (450–750 nm) with 2-order-of-magnitude increase in light emission intensity," *Jpn. J. Appl. Phys.*, vol. 46, no. 4B, pp. 2474–2480, Apr. 2007, doi: 10.1143/JJAP.46.2474.

[4] B. Huang, X. Zhang, W. Wang, Z. Dong, N. Guan, Z. Zhang, and H. Chen, "CMOS monolithic optoelectronic integrated circuit for on-chip optical interconnection," *Opt. Commun.*, vol. 284, nos. 16–17, pp. 3924–3927, Aug. 2011, doi: 10.1016/j.optcom.2011.04.028.

[5] A. Khanmohammadi, R. Enne, M. Hofbauer, and H. Zimmermann, "Monolithically integrated optical random pulse generator in high voltage CMOS technology," in *Proc. 45th ESSDERC*, Sep. 2015, pp. 138–141, doi: 10.1109/ESSDERC.2015.7324732.

[6] K. Xu, "Silicon light-emitting device in standard CMOS technology," in *8th Int. Photon. Opto Electron. Meetings, OSA Tech. Dig.*, Jun. 2015, p. OT1C.3, doi: 10.1364/OEDI.2015.OT1C.3.

[7] S. Dutta, R. Hueting, V. Agarwal, and A.-J. Annema, "An integrated optical link in 140 nm SOI technology," in *Proc. Conf. Lasers Elect.-Opt.*, Jun. 2016, p. 132, doi: 10.1364/CLEO_AT.2016.JW2A.132.

[8] S. Dutta, V. Agarwal, R. J. E. Hueting, J. Schmitz, and A.-J. Annema, "Monolithic optical link in silicon-on-insulator CMOS technology," *Opt. Exp.*, vol. 25, no. 5, pp. 5440–5456, Mar. 2017, doi: 10.1364/OE.25.005440.

[9] A. G. Chynoweth and K. G. Mckay, "Photon emission from avalanche breakdown in silicon," *Phys. Rev.*, vol. 102, no. 2, pp. 369–376, Apr. 1956, doi: 10.1103/PhysRev.102.369.

[10] S. Dutta, R. J. E. Hueting, A.-J. Annema, L. Qi, L. K. Nanver, and J. Schmitz, "Opto-electronic modeling of light emission from avalanche-mode silicon p$^+$n junctions," *J. Appl. Phys.*, vol. 118, p. 114506, Sep. 2015, doi: 10.1063/1.4931056.

[11] P. I. Kuindersma, T. Hoang, J. Schmitz, M. N. Vijayaraghavan, M. Dijkstra, W. van Noort, T. Vanhoucke, W. C. M. Peters, and M. C. J. C. M. Kramer, "The power conversion efficiency of visible light emitting devices in standard BiCMOS processes," in *Proc. 5th IEEE Int. Conf. Group IV Photon.*, Sep. 2008, pp. 256–258, doi: 10.1109/GROUP4.2008.4638164.

[12] G. J. Rees and J. P. R. David, "Nonlocal impact ionization and avalanche multiplication," *J. Phys. D, Appl. Phys.*, vol. 43, p. 243001, Jun. 2010, doi: 10.1088/0022-3727/43/24/243001.

[13] J. W. Slotboom, G. Streutker, M. J. van Dort, P. H. Woerlee, A. Pruijmboom, and D. J. Gravesteijn, "Non-local impact ionization in silicon devices," in *IEDM Tech. Dig.*, Dec. 1991, pp. 127–130, doi: 10.1109/IEDM.1991.235484.

[14] P. Agarwal, M. J. Goossens, V. Zieren, E. Aksen, and J. W. Slotboom, "Impact ionization in thin silicon diodes," *IEEE Electron Device Lett.*, vol. 25, no. 12, pp. 807–809, Dec. 2004, doi: 10.1109/LED.2004.838557.

[15] G. A. M. Hurkx, D. B. M. Klaassen, and M. P. G. Knuvers, "A new recombination model for device simulation including tunneling," *IEEE Trans. Electron Devices*, vol. 39, no. 2, pp. 331–338, Feb. 1992, doi: 10.1109/16.121690

[16] J. J. Liou, "Modeling the tunnelling current in reverse-biased p/n junctions," *Solid-State Electron.*, vol. 33, no. 7, pp. 971–972, Jul. 1990, doi: 10.1016/0038-1101(90)90081-O.

[17] R. Van Overstraeten and H. De Man, "Measurement of the ionization rates in diffused silicon $p - n$ junctions," *Solid-State Electron.*, vol. 13, no. 1, pp. 583–608, May 1970, doi: 10.1016/0038-1101(70)90139-5.

[18] R. F. Pierret, *Semiconductor Device Fundamentals*, Reading, MA, USA: Addison-Wesley, 1996.

[19] *Sentaurus TCAD, Version L-2016.03*, Synopsys Inc., Mountain View, CA, USA, 2016.

[20] M. Lundstrom, *Fundamentals of Carrier Transport*. 2nd ed. Cambridge, U.K.: Cambridge Univ. Press, 2000.

[21] M. Lahbabi, A. Ahaitouf, M. Fliyou, E. Abarkan, J.-P. Charles, A. Bath, A. Hoffmann, S. E. Kerns, and D. V. Kerns, Jr., "Analysis of electroluminescence spectra of silicon and gallium arsenide $p - n$ junctions in avalanche breakdown," *J. Appl. Phys.*, vol. 95, no. 4, pp. 1822–1828, Feb. 2004, doi: 10.1063/1.1326038.

[22] L. W. Snyman, J.-L. Polleux, K. A. Ogudo, C. Viana, and S. Wahl, "High-intensity 100-nW 5 GHz silicon avalanche LED utilizing carrier energy and momentum engineering," *Proc. SPIE*, vol. 8990, p. 89900L, Mar. 2014, doi: 10.1117/12.2038195.

[23] L. W. Snyman, K. Xu, J.-L. Polleux, K. A. Ogudo, and C. Viana, "Higher intensity SiAvLEDs in an RF bipolar process through carrier energy and carrier momentum engineering," *IEEE J. Quantum Electron.*, vol. 51, no. 7, Jul. 2015, Art. no. 3200110, doi: 10.1109/JQE.2015.2427036.

[24] L. W. Snyman, J.-L. Polleux, and K. Xu, "Stimulation of 450, 650 and 850-nm optical emissions from custom designed silicon LED devices by utilizing carrier energy and carrier momentum engineering," *Proc. SPIE*, vol. 10036, p. 1003603, Feb. 2017, doi: 10.1117/12.2264197.

[25] K. R. C. Mok, L. Qi, A. H. G. Vlooswijk, and L. K. Nanver, "Self-aligned two-layer metallization with low series resistance for litho-less contacting of large-area photodiodes," *Solid-State Electron.*, vol. 111, pp. 210–217, Jun. 2015, doi: 10.1016/j.sse.2015.06.011.

[26] K. Xu, Q. Yu, and G. Li, "Increased efficiency of silicon light-emitting device in standard Si-CMOS technology," *IEEE J. Quantum Electron.*, vol. 51, no. 8, Aug. 2015, Art. no. 3000106, doi: 10.1109/JQE.2015.2449759.

[27] S. M. Sze and K. K. Ng, *Physics of Semiconductor Devices*, 3rd ed. New York, NY, USA: Wiley, 2007.

[28] A. Chatterjee and B. Bhuva, "High speed, high reliability Si-based light emitters for optical interconnects," in *Proc. IEEE Int. Interconnect Technol. Conf.*, Jun. 2002, pp. 86–88, doi: 10.1109/IITC.2002.1014896.

[29] P. K. Gopi, G. P. Li, G. J. Sonek, J. Dunkley, D. Hannaman, J. Patterson, and S. Willard, "New degradation mechanism associated with hydrogen in bipolar transistors under hot carrier stress," *Appl. Phys. Lett.*, vol. 63, no. 9, pp. 1237–1239, Aug. 1993, doi: 10.1063/1.109783.

[30] B. K. Boksteen, S. Dhar, A. Ferrara, A. Heringa, R. J. E. Hueting, G. E. J. Koops, C. Salm, and J. Schmitz, "On the degradation of field-plate assisted RESURF power devices," in *IEDM Tech. Dig.*, Dec. 2012, pp. 311–314, doi: 10.1109/IEDM.2012.6479036.

[31] S. Dutta, P. G. Steeneken, V. Agarwal, J. Schmitz, A.-J. Annema, and R. J. E. Hueting, "The avalanche-mode superjunction LED," *IEEE Trans. Electron Devices*, vol. 64, no. 4, pp. 1612–1618, Apr. 2017, doi: 10.1109/TED.2017.2669645.